

# Electron paramagnetic resonance in doped EuO

M. I. Auslender and N. A. Viglin

*Institute of Metal Physics, Ural Science Center, Academy of Sciences of the USSR*

(Submitted 14 February 1986)

Zh. Eksp. Teor. Fiz. **92**, 118–125 (January 1987)

Electron paramagnetic resonance is investigated for specimens of europium monoxide (a magnetic semiconductor) doped with oxygen vacancies, gadolinium, or samarium. The experimental data show that localized electrons in the doped material are primarily responsible for the change in the EPR parameters (there is a shift in the effective  $g$ -factor, and the temperature coefficient of the line width is altered). These electrons form magnetic impurity states whose proper  $g$ -factor differs greatly from 2. Theoretical estimates indicate that a contribution from the conduction electrons should be observable in specimens with carrier concentrations  $\geq 5 \cdot 10^{20} \text{ cm}^{-3}$ .

## I. INTRODUCTION

Europium monoxide (EuO) belongs to a family of materials with unique magnetic, electric, magneto-optic, and microwave properties. Experimental results for monochalcogenides of the type EuX are discussed quite fully in Ref. 1 and have been reviewed in Refs. 2–4; in addition, several chapters in Nagaev's monograph<sup>5</sup> are devoted to an up-to-date theoretical discussion. Nevertheless, little work has been done in certain areas, such as electron paramagnetic resonance (EPR) in EuO. This is because EuO is a magnetically concentrated material and is thus of little interest from the standpoint of EPR spectroscopy, as it possesses only a single, rather broad line ( $\Delta H \sim 10^2\text{--}10^3 \text{ Oe}$ ). However, EPR can be used to study how the magnetic ions interact with the charge carriers that are generated in EuO upon doping with oxygen vacancies or rare-earth metals (Gd, Sm).<sup>2–4</sup>

Doped EuO contains several types of magnetic moments; these include the moments associated with the  $\text{Eu}^{+2}$  ions making up the magnetic matrix of the compound, the magnetic moments of the doping rare-earth metals, and the magnetic moments of the conduction electrons. The high concentration of paramagnetic  $\text{Eu}^{+2}$  ions ( $T > T_c$ ) and the strength of the  $s(d) - f$  exchange interaction between the carriers and the  $\text{Eu}^{+2}$  ions precludes EPR and relaxation of the  $\text{Eu}^{+2}$  moments of the type described by the Korringa theory, and resonance involving the impurity centers or conduction electrons is not observed at rf frequencies. Since only EPR involving the ions in the magnetic matrix is observed, the effect of the doping is to alter the  $g$ -factor and the line width as the doping concentration increases.

EPR in undoped EuO and the dependence of the EPR parameters on doping concentration were first studied experimentally in Refs. 6. The purpose of the present work is to extend these investigations and give a systematic qualitative discussion of the experimental findings. The available information regarding the band structure and the structure of the donor centers in EuX unfortunately does not suffice to permit the development of a quantitative theory.

## 2. EXPERIMENTAL METHOD AND RESULTS

In the experiments we employed an ER-9 EPR spectrometer and an ERS-230 x-ray spectrometer (both are available commercially); they were equipped with a thermostat for regulating the temperature to within 1 K,

$100 \leq T \leq 400 \text{ K}$ . The EuO single- and polycrystal specimens were doped with Gd and Sm to 2 at. % and contained various amounts of excess Eu.

Because the compounds EuX are highly ionic and the "lanthanoid compression"<sup>2</sup> is pronounced,  $\text{Eu}_{1-x}\text{R}_x\text{O}$  solid solutions obey the Vegard law and x-ray spectroscopy can be used to determine the concentration  $x$  with high accuracy. This method was used to find  $x$  for our specimens (these measurements were carried out by M. I. Simonova and N. M. Chebotayev.) No comparably precise method is available for measuring the vacancy concentration ( $x$ ) in  $\text{EuO}_{1-x}$ . In particular, values of  $x$  deduced from the vacancy IR absorption line are only approximate. The latter method was used in Ref. 7, where  $\text{EuO}_{1-x}$  specimens with physical properties similar to ours were grown under comparable conditions; we will use these values below.

The highly conductive specimens ( $\sigma > 1 \Omega^{-1} \cdot \text{cm}^{-1}$ ) were ground into a powder in order to avoid distortion of the lineshape from symmetry caused by the skin effect. The grain size was monitored in terms of the distortion. The powder was imbedded in paraffin, which served to electrically isolate the particles; this technique is described in detail in Ref. 8. We merely note that the surface defects produced during the pulverization apparently did not alter the relaxation processes significantly, since in poorly conducting specimens ( $\sigma < 1 \Omega^{-1} \cdot \text{cm}^{-1}$ ) the resonance field and the shape and width of the line were identical (to within the experimental error) for the powders and for the starting single crystals. We used the four-probe method to measure the dc electric conductivity of the single crystals. Measurements

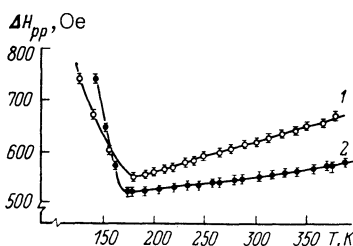


FIG. 1. Temperature dependence of the EPR linewidth in specimens with metallic conduction: 1)  $\text{Eu}_{1-x}\text{Gd}_x\text{O}$ , specimen No. 5; 2)  $\text{Eu}_{1-x}\text{Sm}_x\text{O}$ , specimen No. 9.

TABLE I. Specimens with nearly stoichiometric compositions. <sup>1</sup>

Specimen	$\sigma, \Omega^{-1} \cdot \text{cm}^{-1}$	$n, \text{cm}^{-3}$	$g$	$\gamma, \text{Oe}/\kappa$
1. EuO	$10^{-7}$	—	1.99(5)	0.15
2. EuO	$10^{-7}$	—	1.99(5)	0.15
3. EuO	$1.2 \cdot 10^{-7}$	—	1.99	0.3

based on the Hall effect were used to find the concentration  $n$  of conduction electrons for specimens with  $\sigma > 10^{-5} \Omega^{-1} \cdot \text{cm}^{-1}$ .

The experimental results are shown in Fig. 1 and in Tables I–III. We divide the specimens into three groups—those with nearly stoichiometric compositions (highly resistive,  $\sigma \sim 10^{-7} \Omega^{-1} \cdot \text{cm}^{-1}$ ), doped specimens behaving as semiconductors, and specimens exhibiting metallic conduction. Figure 1 shows the temperature dependence  $\Delta H(T)$  of the line width for two metallic specimens,  $\text{Eu}_{1-x}\text{Gd}_x\text{O}$  (1) and  $\text{Eu}_{1-x}\text{Sm}_x\text{O}$  (2). These curves are in fact typical for all single-phase specimens (i.e., when no  $\text{Eu}_3\text{O}_4$  phase is present)<sup>6</sup>:  $\Delta H(T)$  drops steeply as  $T$  increases from  $\sim \theta$  (where  $\theta$  is the paramagnetic Curie temperature) until  $T$  reaches a value  $T_{\min}$ , after which  $\Delta H(T)$  increases almost linearly over a large interval extending up to 400 K. For  $T > T_{\min}$  the curves can thus be characterized by their slope  $\gamma = d\Delta H/dT$ , which is listed in the last column in Table I–III.

**Line widths.** Our measured widths  $\Delta H$  are in complete agreement with the results found in Refs. 6. Doping changes the values of  $\Delta H_{\min} = \Delta H(T_{\min})$  and  $\gamma$ . The drop in  $\Delta H_{\min}$  with increasing doping concentration is pronounced for Gd and Sm but extremely slight for the case of oxygen vacancies; the indirect exchange theory<sup>1,5</sup> was used in Refs. 6 to explain this behavior. The value of  $\gamma$  at first increases; after the semiconductor-metal transition has occurred,  $\gamma$  decreases in some of the  $\text{Eu}_{1-x}\text{Gd}_x\text{O}$  ( $\text{Eu}_{1-x}\text{Sm}_x\text{O}$ ) specimens but falls off only slightly in  $\text{EuO}_{1-x}$ . Moreover, for some of the  $\text{Eu}_{1-x}\text{Gd}_x(\text{Sm}_x)\text{O}$  specimens (Nos. 1–3, 5–7 in Table III),  $\gamma$  actually increases after the semiconductor-metal transition. We will discuss the reasons for this below.

**Effective  $g$  factor.** The  $g$ -factor is defined as usual by

$$g = \hbar\omega / \mu_B H_r, \quad \omega = 2\pi f, \quad (1)$$

where  $f$  is the oscillator frequency,  $\mu_B$  is the Bohr magneton, and  $H_r$  is the resonance field. Our measured values for  $g$  are accurate only to two decimal places, and the scatter in the  $\gamma$  values for some of the specimens is due to random lineshape distortions having no influence on the resonance field. The difference  $g_0 - g$  has the same general behavior as  $\gamma$  (here  $g_0 \approx 1.99$  is the  $g$ -factor for  $\text{Eu}^{2+}$  and  $\text{Gd}^{2+}$  in a cubic crystal

with an octahedral nearest-neighbor configuration<sup>9</sup>). Before the semiconductor-metal transition,  $g_0 - g$  also increases with doping concentration from 0 to 0.02–0.03, while after the transition it decreases almost to zero in the same  $\text{Eu}_{1-x}\text{Gd}_x(\text{Sm}_x)\text{O}$  compounds for which  $\gamma$  is found to decrease. On the other hand,  $g_0 - g$  remains well away from zero ( $\sim 0.02 - 0.03$ ) for those metallic  $\text{EuO}_{1-x}$  and  $\text{Eu}_{1-x}\text{Gd}_x(\text{Sm}_x)\text{O}$  specimens for which  $\gamma$  is large ( $\sim 0.7-0.9 \text{ Oe}/\text{K}$ ).

### 3. THEORETICAL DISCUSSION

In view of the strength of the  $f$ - $d$  exchange interaction for  $\text{Eu}^{+2}$  and  $\text{Gd}^{+2}$  ions (for which  $I_0 = 0.195$  and  $0.250 \text{ eV}$ , respectively),<sup>1</sup> we may assume that the EPR in doped EuO has a “bottleneck” in which the rate-limiting process involves the excitation of the transverse components of the total moment

$$\mathbf{S}_i = \mathbf{S} + \mathbf{S}_e, \quad (2)$$

where  $\mathbf{S}$  is the total moment of the rare-earth spin subsystem and  $\mathbf{S}_e$  is the total moment of the carriers. The technique due to Mori in the theory of magnetic resonance and relaxation<sup>10</sup> can be used to calculate the contribution from the carriers to the  $g$ -factor and the EPR line width when  $\hbar\omega \ll k_B T$ . We have

$$g - g_0 = (g_e - g_0) \langle \mathbf{S}_i \mathbf{S}_e \rangle / \langle \mathbf{S}_i^2 \rangle, \quad (3)$$

$$(\Delta H)_e = \gamma_e(T) (T - \theta),$$

$$T\gamma_e(T) \approx \frac{1}{NS(S+1)\mu_B} \int_0^\infty dt \langle \dot{\mathbf{S}}_e(t) \dot{\mathbf{S}}_e(0) \rangle, \quad (4)$$

where  $g_e$  is the spectroscopic splitting factor for the carriers,  $N$  is the number of sites in the rare-earth sublattice,  $S = 7/2$ , and  $\dot{\mathbf{S}}_e$  is the time derivative of the moment operator for the carriers (it gives the change in the moment due to relativistic interactions with the lattice). The experimental data imply that for our specimens, the dominant spin-lattice relaxation processes are the ones for which

$$\gamma_e(T) \approx \gamma_e = \text{const}(T) \text{ for } T \gg \theta. \quad (5)$$

We have  $g \approx g_0$  and  $\gamma \lesssim 0.3 \text{ Oe}/\text{K}$  for the nearly stoichiometric (Table I) and weakly doped specimens (Table II, No. 1).

TABLE II. Doped semiconducting specimens.

Specimen	$x, \text{at.}\%$	$\sigma, \Omega^{-1} \cdot \text{cm}^{-1}$	$n, \text{cm}^{-3}$	$g$	$\gamma, \text{Oe}/\kappa$
1. $\text{EuO}_{1-x}$	—	$1.2 \cdot 10^{-5}$	$6.8 \cdot 10^{12}$	1.99(0)	0.25
2. $\text{EuO}_{1-x}$	$\sim 0.35$	$4 \cdot 10^{-5}$	$2 \cdot 10^{13}$	1.98	0.6
3. $\text{Eu}_{1-x}\text{Gd}_x\text{O}$	$0.55 \pm 0.02$	$5 \cdot 10^{-5}$	—	1.98	0.6
4. $\text{Eu}_{1-x}\text{Gd}_x\text{O}$	$0.15 \pm 0.02$	$2 \cdot 10^{-4}$	$10^{14}$	1.99	$0.14-0.2$
5. $\text{Eu}_{1-x}\text{Gd}_x\text{O}$	$0.90 \pm 0.02$	$3 \cdot 10^{-4}$	—	1.97(5)	0.8
6. $\text{EuO}_{1-x}$	—	$1.4 \cdot 10^{-3}$	$9 \cdot 10^{14}$	1.96	1.1
7. $\text{EuO}_{1-x}$	$\sim 0.4$	$5 \cdot 10^{-3}$	$3 \cdot 10^{15}$	1.96	1.1

TABLE III. Specimens with metallic conduction.

Specimen	$x$ , at. %	$\sigma$ , $\Omega^{-1} \cdot \text{cm}^{-1}$	$n$ , $\text{cm}^{-3}$	$g$	$\gamma$ , Oe/ $\kappa$
1. $\text{Eu}_{1-x}\text{Sm}_x\text{O}$	—	33	$10^{19}$	1.98	1.0
2. $\text{EuO}_{1-x}$	$\sim 0.5$	50	$2.5 \cdot 10^{19}$	1.96	0.8
3. $\text{Eu}_{1-x}\text{Sm}_x\text{O}$	—	$1.7 \cdot 10^2$	$8.8 \cdot 10^{19}$	1.98	0.9
4. $\text{Eu}_{1-x}\text{Gd}_x\text{O}$	$1.13 \pm 0.02$	$10^3$	$10^{20}$	1.99 (4)	0.35–0.5
5. $\text{Eu}_{1-x}\text{Gd}_x\text{O}$	$1.31 \pm 0.02$	$10^3$	$2 \cdot 10^{20}$	1.96 (6)	0.8–0.9
6. $\text{Eu}_{1-x}\text{Gd}_x\text{O}$	—	$4 \cdot 10^2 - 10^3$	$2 \cdot 10^{20}$	1.97	0.8–0.9
7. $\text{Eu}_{1-x}\text{Gd}_x\text{O}$	—	$10^3$	$4 \cdot 10^{20}$	1.98	0.7
8. $\text{Eu}_{1-x}\text{Gd}_x\text{O}$	$1.60 \pm 0.02$	$1.25 \cdot 10^3$	$5 \cdot 10^{20}$	1.99	0.4–0.5
9. $\text{Eu}_{1-x}\text{Sm}_x\text{O}$	—	$1.25 \cdot 10^3$	$5.5 \cdot 10^{20}$	1.99	0.4–0.5
10. $\text{Eu}_{1-x}\text{Gd}_x\text{O}$	$1.58 \pm 0.02$	$10^3$	$6 \cdot 10^{20}$	1.99 (4)	0.35

We note that there are no specimens for which  $\gamma < 0.14$  Oe/K, which suggests that there is an “intrinsic” contribution  $-\Delta H_0$  to the line width which is proportional to the temperature:  $\gamma_0 = d\Delta H_0/dT \sim 0.15-0.2$  Oe/K. This contribution could be due to phonon modulation of the crystal and dipole fields.<sup>6</sup>

The data in Tables II and III show that as already noted (Sec. 2), the EPR parameters depend appreciably on the doping concentration and on the departure from stoichiometry. Recourse to experimental results regarding the impurity states and impurity conduction band in EuO is necessary in order to explain this qualitatively.

The excess electrons in  $\text{EuO}_{1-x}$  are located near the oxygen vacancies, and the observed activation energy for conduction is equal to 0.3 eV for all  $x \lesssim 0.35\%$  ( $T > 100$  K), while the semiconductor-metal transition occurs when  $x = x_c \sim 0.4\%$  (Refs. 4, 7). Although it is widely assumed that each  $\text{Gd}^{+2}$  ( $4f^7 5d^1$ ) ion concentrations a  $5d$ -electron to the impurity state in materials doped with Gd ( $4f^7 5d^1 6s^2$ ),<sup>1-4</sup> conflicting results have been obtained concerning the energy levels. For example, in their elaborate numerical analysis of data on the magneto-optical effects associated with the free carriers, Schoens and Wachter<sup>4</sup> concluded that the Gd donor level in EuO lies at a depth of 0.017 eV. On the other hand, direct measurements on a large number of  $\text{Eu}_{1-x}\text{Gd}_x\text{O}$  specimens grown under various conditions imply an activation energy of 0.4 eV (just as for  $\text{Eu}_{1-x}\text{Gd}_x\text{Se}$ ), while near the semiconductor-metal transition ( $x_c \approx 1.1\%$ ) the minimum activation energy is equal to 0.27 eV (Refs. 11, 12).

In  $\text{Eu}_{1-x}\text{Sm}_x\text{O}$  the impurity state forms when a local electron transition changes the valence of the samarium ion,  $\text{Sm}^{+2}(4f^6) \rightarrow \text{Sm}^{+3}(4f^5)$  (this transition can be observed in the  $L_{III}$  x-ray absorption spectra<sup>13</sup>). The activation energy and the critical concentration  $x_c$  for  $\text{Eu}_{1-x}\text{Sm}_x\text{O}$  are roughly the same as for  $\text{Eu}_{1-x}\text{Gd}_x\text{O}$  (Ref. 11).

Although the impurity states are different, measurements of the thermal  $\text{emf}^{11}$  indicate that the density of states in the impurity conduction bands is characterized by the same effective mass  $m_d = 1.1 m_0$  for all the heavily doped  $\text{EuO}_{1-x}$ ,  $\text{Eu}_{1-x}\text{Gd}_x\text{O}$ , and  $\text{Eu}_{1-x}\text{Sm}_x\text{O}$  specimens, in good agreement with the results obtained in Ref. 14 from energy band calculations for EuO. Analysis of data on the red shift of the optical absorption edge for  $\text{Eu}_{1-x}\text{Gd}_x\text{O}$  (Ref. 15) yields the same mass  $m_d$ . Nevertheless, the free energy concentrations  $n$  deviate appreciably from the doping concentration  $x/v_0$ , where  $v_0 = a^3/4$  is the volume of the EuO unit cell, for all but the most heavily doped metallic  $\text{Eu}_{1-x}\text{Gd}_x(\text{Sm}_x)\text{O}$  specimens (Nos. 8–10 in Table III).

The deviation is particularly pronounced (roughly an order of magnitude) for metallic  $\text{EuO}_{1-x}$  (Table III, No. 2), whose conduction electron concentration is the maximum possible for nonstoichiometric EuO when  $T > T_c$ .

We will first estimate the contribution from the conduction electrons to the EPR parameters for the metallic specimens ( $x > x_c$ ). The experimental data in Refs. 11 and 12 indicate that the carriers are degenerate for the temperatures of interest. The averages in (3) can be calculated by applying degenerate perturbation theory (small  $d$ - $f$  exchange parameter<sup>5</sup>) to the standard parabolic band model. We have

$$g - g_0 \approx (\delta g_e) \frac{I_0 m v_0}{4\pi \hbar^2} \left( \frac{3}{\pi} n \right)^{1/2} \approx 0.74 (\delta g_e) \cdot 10^{-2} v^{1/2},$$

$$\delta g_e = (g_e - 2), \quad v = n \cdot 10^{-21} \text{ cm}^3, \quad (6)$$

where the estimates are accurate to 1 part in  $10^4$  and the numerical values  $I_0 = 0.2$  eV,  $m = m_d = 1.1 m_0$ ,  $a = 5.13 \text{ \AA}$  have been assumed. The value of  $\gamma_e$  is determined primarily by impurity and phonon scattering of the conduction electrons accompanied by spin flip; these scattering mechanisms are discussed in detail in Ref. 16 for ordinary semiconductors. Only impurity scattering satisfies the condition (5).<sup>17</sup> Calculating  $\gamma_e$  under the above assumptions and using the symmetry of the edge of the conduction band for EuO (Ref. 14), we obtain

$$\gamma_e = \Lambda^2 x_i (Ze^2/\kappa_0)^2 (12\pi m^2 v_0^{1/3} k_B / \hbar^4 S(S+1) \mu_B)$$

$$\times \left( \frac{3n}{\pi} \right)^{3/2} F \left( \frac{2\pi^2 \hbar^2 \kappa_0}{m e^2} \left( \frac{3}{\pi} n \right)^{1/2} \right)$$

$$\approx 1.82 (\delta g_e)^2 10^3 x_i Z^2 v^{3/2} F(24.5 v^{1/2}) \text{ Oe/K}, \quad (7)$$

where the parameter  $\Lambda$  characterizes the spin-orbit mixing of band states with opposite spin projections ( $\Lambda \approx |\delta g_e|$ , Ref. 16);  $x_i = n v_0$  is the concentration of impurity ions, with effective charge  $Z$ ;  $\kappa_0$  is the static dielectric constant ( $\kappa_0 = 24$  for EuO, Ref. 4), and

$$F(u) = (1 + 2u^{-1}) \ln(1 + u) - 2.$$

For the two  $\text{Eu}_{1-x}\text{Gd}_x\text{O}$  specimens (8 and 10 in Table III), the contribution  $\gamma_e = \gamma - \gamma_0 \approx 0.2-0.8$  Oe/K may be attributed to the conduction electrons, since in this case  $x_i = x$ . The same is apparently also true for metallic  $\text{Eu}_{1-x}\text{Sm}_x\text{O}$  (specimen No. 9). Setting  $\gamma_e \sim 0.2-0.3$  Oe/K,  $x_i = 1.6 \cdot 10^{-2}$ ,  $Z = 1$ , and  $v = 0.5-0.6$  in (7), we find that

$$|\delta g_e| \sim 0.1. \quad (8)$$

With this estimate, (6) gives the bound

$$|g - g_0| \leq 10^{-3}, \quad (9)$$

for the shift in the  $g$ -factor for these specimens, in agreement with the experimental data (specimens 8–10 in Table III). We note that the result (8) is quite plausible if Elliot's estimate<sup>16</sup>

$$|\delta g_e| \sim \lambda / \Delta E \quad (10)$$

remains valid for an impurity band, in which case  $\Delta E$  should be comparable to the band width. Since the spin-orbit interaction constant  $\lambda$  for the  $5d$ -electrons in  $\text{Eu}^{+2}$  and  $\text{Gd}^{+2}$  is of the order of 0.1 eV (Ref. 1), the estimates (8) and (10) imply that  $\Delta E \sim 0.1$  eV, in agreement with the effective mass ( $\Delta E \sim \hbar^2 K_{\text{max}}^2 / 2m$ ).

The estimates (7)–(9) and the experimental data on  $n$  indicate that for specimens 1–7 the conduction electrons can alter the EPR parameters only slightly, by less than the experimental error. Thus for specimens with  $x < x_c$ , and also for metallic specimens in which the concentration of impurity centers differs appreciably from the free carrier concentration, localized states filled with electrons must be responsible for the observed changes in the EPR parameters. It is clear from Eq. (3) that these states must be quite deep, i.e.,  $|\delta g_e|$  is  $\sim 1$  [on the other hand, the estimate (8) is reasonable for shallow states]. Although the mechanism by which these states are generated must clearly depend on how the materials are doped, it seems likely that localization within clusters is involved in all cases. In  $\text{EuO}_{1-x}$ , for example, the donor electrons are actually localized not at the centers but within clusters of Eu ions surrounding a vacancy. Since no decrease in the activation energy is observed even for  $x \sim 0.35\%$ , there can be little overlap among these states even when  $x$  becomes quite large.<sup>7,11</sup> The large difference between  $n$  and  $x/\nu_0$  noted above indicates that even after the semiconductor-metal transition occurs, a substantial fraction of the electrons remain in localized (Anderson) states. Our EPR data suggest indirectly that deep states in the  $\text{EuO}_{1-x}$  impurity band are also important when  $x > x_c$ . This can be explained qualitatively as follows. Owing to the highly ionic nature of the compound  $\text{EuO}$ , as the free carrier concentration rises the increase in the energy of the metallic bonds eventually fails to offset the loss in the electrostatic energy caused by local deviations from electrical neutrality.

Clusters can also form in specimens doped with Gd or Sm. Indeed, either excess metal or excess oxygen may be present in  $\text{Eu}_{1-x}\text{R}_x\text{O}$  solid solutions grown by the standard techniques.<sup>1-4</sup> In the first case the clusters are centered around oxygen vacancies, while in the second case they contain both  $\text{Eu}^{+2}$  and  $\text{Eu}^{+3}$  ions (the latter are produced together with europium vacancies<sup>4,7</sup>). The impurity state formed by a Gd or Sm ion in such a cluster will differ from the donor Gd or Sm states in a stoichiometric environment. The latter probably correspond to the "shallow" states in  $\text{Eu}_{1-x}\text{Gd}_x\text{O}$  which have been observed in optical experiments but which are masked in transport experiments by deep states in the clusters. Beyond the semiconductor-metal transition,  $x$  and  $x_i$  for  $\text{Eu}_{1-x}\text{Gd}_x\text{O}$  are more nearly equal than for  $\text{EuO}_{1-x}$  ( $x_i \sim 0.5x$  for specimens 4 and 5 in Table III). The EPR experiments for  $\text{Eu}_{1-x}\text{Gd}_x(\text{Sm}_x)\text{O}$  for  $x > x_c$  show that below the mobility threshold, either shallow states (specimen 4) or deep states (specimens 1, 3, 5–7)

may dominate in these materials. The shallow states have little influence on  $\gamma$  and contribute imperceptibly to  $g_0 - g$ .

A similar situation may also be observed when  $x < x_c$ . Indeed, the doping concentration for specimen 4 in Table II was too low to affect the EPR parameters. Nevertheless, its conductivity was four times greater than for the more heavily doped  $\text{Eu}_{1-x}\text{Gd}_x\text{O}$  (specimen 3), and was almost the same as for specimen 5, for which  $x$  was near the critical value for the semiconductor-metal transition. Possibly, the impurity in specimen 4 remained as individual ions, while in specimens 3 and 5 many of the ions were present in clusters. We have already noted that the europium vacancies in these clusters are not acceptors in the usual sense; however, they should have significant compensating properties and appreciably decrease the conductivity of the specimens.

Since the structure of the impurity state is not known, we consider a very simple generalization of the Kasuya-Yanase model.<sup>18</sup> The  $d$ -electron in the magnetic impurity state is assumed to move in the slightly distorted field of the octahedral complex, and we use the simple term

$$-\Delta_e S_e s \quad (11)$$

to describe the exchange interaction between an electron of spin  $s$  and the  $\text{Eu}^{+2}$  ions in a cluster. Here  $\Delta_e$  is the average  $d$ - $f$  exchange parameter inside the cluster, whose total spin is  $S_e$ . We assume that we have the inequalities

$$\Delta_{s_0} > \Delta_e > \Delta_{cr}, \quad (12)$$

where  $\Delta_{s_0}$  is the spin-orbit splitting and  $\Delta_{cr}$  is the splitting caused by the noncubic component of the crystal field. Using the crystal field theory<sup>9</sup> and the results in Ref. 19, we find from Eq. (3) that

$$g - g_0 = -\frac{k+2}{3} \frac{x_{cl} N_c}{S+1} B_S \left( \frac{\Delta_e S}{k_B (T - \theta_0)} \right), \quad S = 7/2. \quad (13)$$

Here the factor  $0 < k < 1$  allows for the decrease in the orbital momentum due to the fact that the bonds are partially covalent ( $\Delta_{s_0} \sim k$ ),<sup>9</sup>  $x_{cl}$  is the cluster concentration,  $N_c$  is the number of  $\text{Eu}^{+2}$  ions in a cluster,  $B_S$  is the Brillouin function, and  $\theta_0$  is the paramagnetic Curie temperature for stoichiometric  $\text{EuO}$  (Refs. 1–4).

Equation (13) predicts the correct sign ( $g - g_0 < 0$ ), since the contribution of the orbital momentum makes  $g_e$  strictly less than 2. According to (12), we have  $|\delta g_e| \sim 2$ , so that the magnitude of the small difference  $g_0 - g$  depends only on  $x_c$  and  $T$ . The measurements of the paramagnetic susceptibility of  $\text{Eu}_{1-x}\text{Gd}_x\text{O}$  in Ref. 20 yield the estimate  $\Delta_e/k_B \sim 80$  K, which implies that (13) correctly describes the observed difference  $g_0 - g$  if  $x_{cl} \sim 0.5 - 1\%$ . Formula (13) also predicts an increase in  $g_0 - g$  with decreasing temperature. This behavior is in fact observed for all specimens for which  $g_0 - g \gtrsim 10^{-2}$  at room temperature. Unfortunately, it is difficult to distinguish this effect, which is due to an increase in the local spin of the clusters, from the effects of magnetization reversal, which become significant even for  $T \sim 200$  K owing to the "tail" in the magnetization curve (since  $H \neq 0$ ).

We observe in closing that the large values of  $\gamma$  for these specimens (Nos. 3–7 in Table II and 5–7 in Table III) are probably caused by the spin-lattice relaxation of the impuri-

ty electrons in the clusters that accompanies the phonon modulation of the crystal fields. Indeed, the interaction (11) splits the energy level of an electron bound to an impurity into numerous sublevels with spacing  $\Delta_e < k_B T$  (Ref. 18) and thereby enhances the Orbach relaxation,<sup>9</sup> for which (5) is satisfied.

We are deeply grateful to A. A. Samokhvalov for his unflinching interest in this work.

<sup>1</sup>S. Methfessel and D. C. Mattis, "Magnetic semiconductors," in: *Handbuch der Physik* (ed. by H. P. J. Wijn), Vol. 18, Part 1, Springer Verlag, New York (1968), pp. 389–562.

<sup>2</sup>Fizicheskie Svoistva Khal'kogenidov Redkozemel'nykh Elementov (Physical Properties of Rare-Earth Chalcogenides), A. V. Golubkov *et al.* eds., Nauka, Leningrad (1973).

<sup>3</sup>A. A. Samokhvalov, in: *Redkozemel'nye Poluprovodniki* (Rare-Earth Semiconductors), V. P. Zhuze and I. A. Smirnov eds., Nauka, Leningrad (1977), p. 5.

<sup>4</sup>P. Wachter, in: *CRC Crit. Rev. Solid State Sci.* **3**, 189 (1972); P. Wachter, in: *Handbook on Phys. of Rare Earths* (K. A. Gschneider Jr. and L. Eyring eds.), North-Holland, Amsterdam (1979), p. 507.

<sup>5</sup>É. L. Nagaev, *Fizika Magnitnykh Poluprovodnikov* (Physics of Magnetic Semiconductors), Nauka, Moscow (1979).

<sup>6</sup>A. A. Samokhvalov and V. S. Babushkin, *Fiz. Tverd. Tela* **12**, 13 (1970) [*Sov. Phys. Solid State* **12**, 9 (1970)]; A. A. Samokhvalov, N. A. Viglin, B. A. Gizhevskii, *et al.*, *Fiz. Tverd. Tela* **23**, 870 (1981) [*Sov. Phys. Solid State* **23**, 496 (1981)].

<sup>7</sup>M. W. Shafer, J. B. Torrance, and T. Penney, *J. Phys. Chem. Solids* **33**, 2251 (1972).

<sup>8</sup>J. S. Sansonett, D. P. Mullin, J. R. Dixon, and J. K. Furdyna, *J. Appl. Phys.* **50**, 5431 (1979).

<sup>9</sup>A. Abragam and B. Bleaney, *Electron Paramagnetic Resonance of Transition Ions*, Clarendon Press, Oxford (1970).

<sup>10</sup>H. Mori, *Progr. Theor. Phys.* **34**, 435 (1965); D. Kivelson and K. Ogan, *Adv. Magn. Res.* **7**, 72 (1974).

<sup>11</sup>B. A. Gizhevskii, Author's Abstract of Candidate's Dissertation, Sverdlovsk (1983).

<sup>12</sup>C. Godart, A. Mauger, J. P. Desfours, and J. C. Achard, *J. de Phys., Coll. C5, Suppl. No. 6*, 205 (1980).

<sup>13</sup>A. A. Samokhvalov, T. I. Arbuzova, A. Ya. Afanas'ev, *et al.*, *Fiz. Tverd. Tela* **17**, 48 (1975) [*Sov. Phys. Solid State* **17**, 26 (1975)]; A. A. Samokhvalov, T. I. Arbuzova, V. S. Babushkin, *et al.*, *Fiz. Tverd. Tela* **18**, 2830 (1976) [*Sov. Phys. Solid State* **18**, 1655 (1975)].

<sup>14</sup>S. J. Cho, *Phys. Rev.* **131**, 4589 (1970).

<sup>15</sup>N. G. Bebenin, *Solid State Comm.* **55**, 823 (1985).

<sup>16</sup>R. J. Elliot, *Phys. Rev.* **96**, 266 (1954); Y. Yafet, in: *Solid State Phys.* **14**, (D. Turnbull and F. Seitz eds.), New York (1964), p. 1.

<sup>17</sup>N. V. Kozhevnikov, Author's Abstract of Candidate's Dissertation, Sverdlovsk (1980).

<sup>18</sup>T. Kasuya and A. Yanase, *Rev. Mod. Phys.* **40**, 684 (1968); A. Yanase and T. Kasuya, *J. Phys. Soc. Jpn.* **25**, 1025 (1968).

<sup>19</sup>S. M. Ryabchenko and Yu. G. Semenov, *Zh. Eksp. Teor. Fiz.* **84**, 1419 (1983) [*Sov. Phys. JETP* **54**, 825 (1983)].

<sup>20</sup>A. A. Samokhvalov, T. I. Arbuzova, M. P. Simonova, and L. D. Fal'kovskaya, *Fiz. Tverd. Tela* **15**, 3690 (1973) [*Sov. Phys. Solid State* **15**, 2459 (1973)].

Translated by A. Mason